

Proceeding Series of the Brazilian Society of Computational and Applied Mathematics

Orbital evolution of a solar sail around a planet

Jean Paulo dos S. Carvalho¹

Centro de Ciência e Tecnologia em Energia e Sustentabilidade, Universidade Federal do Recôncavo da Bahia, Feira de Santana-BA

Abstract. Solar sails are a type of propulsion that uses solar radiation pressure to generate acceleration. The fundamental goal for any solar sail design is to provide a large, flat reflective film which requires a minimum of structural support mass. In this research is taken into account the non-sphericity of the central body, the perturbation of the third body and the solar radiation pressure to analyze the behavior of the orbit when the artificial satellite is a solar sail around Mercury. We present an approach where we show a section of frozen orbits. A set of initial conditions, which may contribute with the scientific missions planned to visit the planet Mercury the next few years, are presented. Frozen orbits were found, i.e. orbits with less variation of the orbital elements. We show that the parameter of the solar sail that depends, among other factors, the mass per unit area contributes to obtain frozen orbits.

Keywords. Solar sail, Frozen orbits, Third-body perturbation, Solar radiation pressure, Mercury.

1 Introduction

Solar sails are a type of propulsion that uses solar radiation pressure to generate acceleration. They are made of large mirrors, low mass, which gain momentum reflecting photons, the quantum energy packages that light is composed. In theory, these photons will transfer its energy to solar sails, causing the ship to move. The use of propellant systems (without particles material expelled for propulsion) as solar sails in recent days has attracted the interest of scientific missions. The influence of radiation pressure on the solar sail creates an additional force to the dynamics of the problem, and this force must be taken into account, since it can change the behavior of the orbits. This paper presents an approach to dynamic properties of a propulsion system using solar radiation. The model of forces acting on the spacecraft is developed. In this research, an analysis is presented as the solar radiation pressure affects the frozen orbits (orbits are having constant orbital elements on average) around a planet while spacecraft is a solar sail. Thus, the forces considered in the dynamics are non-uniform distribution of mass of the planet, the gravitational perturbation due to the Sun (the third body effect) and the solar radiation pressure. The objective of this work is the computation of frozen orbits to a

¹jeanfeg@gmail.com

solar sail around Mercury. A study of dynamical properties of a propulsion system using solar radiation and an extensive literature review that takes into account a solar sail is presented in [2].

Are displayed a set of initial conditions that were obtained from frozen orbits around Mercury which can contribute to the planning of orbits, for example, for the BepiColombo mission. BepiColombo is a joint mission of the European Space Agency (ESA) and the Japan Aerospace Exploration Agency (JAXA) to exploit the planet Mercury, under the leadership of ESA. The mission entered the implementation phase in early 2007, and its launch is planned for 2017. The BepiColombo mission, comprising two main spacecraft, will still reach Mercury in January 2024. In general, for orbiters around Mercury (see [5]), it is necessary to consider the third-body attraction, that is, the Sun attraction, due to its proximity. If the spacecraft is provided with a large sail, the solar radiation pressure perturbation is worth considering. Thus, we deal with a Hamiltonian characterized by the Kepler problem, Mercury's gravitational potential, the third body perturbation and the solar radiation pressure. We also include the eccentricity and inclination of the orbit of Mercury around the Sun and the oblateness of Mercury caused by the zonal terms J_2 and J_3 .

2 Equations of motion

We consider the planet Mercury around the Sun in an elliptical and inclined orbit to investigate the dynamics of a solar sail type artificial satellite. In [5] the authors show the development of the equations of motion for the problem proposed in this work. Here we present only the basic equations used to obtain the equations of motion. So for more details see the cited papers. Let us consider a $Oxyz$ reference frame centered on the main body, Mercury, the Oxy plane coincides with the planet's equator, the x -axis along the intersection line of the equatorial plane of the main body and the orbital plane of the third body. It is assumed that the third body follows an elliptic and inclined orbit around the main body with semimajor axis a_{\odot} , eccentricity e_{\odot} and inclination i_{\odot} . The spacecraft orbits about the central body with semimajor axis a , eccentricity e , inclination i , right ascension of the ascending node Ω , argument of the pericentre w and mean motion n , and its motion is perturbed by the third body. The motion of the solar sail about Mercury under the gravitational effect of the central body and perturbed by the gravitational attraction of the third body, Sun, and the Solar radiation pressure is described by

$$\ddot{\mathbf{r}} = \ddot{\mathbf{r}}_M + \ddot{\mathbf{r}}_{3b} + \ddot{\mathbf{r}}_{SRP} = \ddot{\mathbf{r}}_M \nabla U_M(\mathbf{r}) - \mu_{\odot} \left(\frac{\mathbf{r} - \mathbf{r}_{\odot}}{\|\mathbf{r} - \mathbf{r}_{\odot}\|^3} + \frac{\mathbf{r}_{\odot}}{\|\mathbf{r}_{\odot}\|^3} \right) + \beta \mu_{\odot} \frac{\mathbf{r} - \mathbf{r}_{\odot}}{\|\mathbf{r} - \mathbf{r}_{\odot}\|^3} \quad (1)$$

for the central planet we only take into account the zonal contribution (U_M). Where \mathbf{r} is the position of the state vector of the spacecraft with respect to the central planet Mercury, μ_{\odot} represents the gravitational parameter of the Sun, and \mathbf{r}_{\odot} is the position vector of the Sun with respect to Mercury. Here $\beta < 1$ is a constant associated to the sail. The dimensionless sail loading parameter β will be defined as the ratio of the solar radiation

pressure acceleration to the solar gravitational acceleration ([3]). With this, we obtain atlases of families of frozen orbits depending on the parameter β . Here $\beta = \frac{L_{\odot}A}{2\pi mGM_{\odot}c}$, where M_{\odot} is the solar mass, G is the universal gravitational constant, L_{\odot} is the Sun's luminosity, m , A are the mass and area of the solar sail, respectively and c is the speed of light.

2.1 Perturbations of the third body and solar radiation pressure

The motion of the sail is studied under the double-averaged analytical model with the aim of reducing the degrees of freedom of the system and eliminate the short-period terms. The double averaged procedure consists of a first average over the period of the sail and second averaging over the period of the third body. After performing the average over the eccentric anomaly of the sail, the equation obtained is

$$\langle R_{3b} \rangle = \frac{3a^2n_{\odot}^2}{4} \left(\frac{a_{\odot}}{r_{\odot}} \right)^3 (\alpha^2(1 + 4e^2) + \gamma^2(1 - e^2) - \left(\frac{2}{3} + e^2 \right)) \quad (2)$$

where n_{\odot} is the mean motion of the third body. Regarding to solar radiation pressure perturbation, the average over the eccentric anomaly of the spacecraft and we obtain the following expression

$$\langle R_{SRP} \rangle = -\beta \frac{3a^2n_{\odot}^2}{4} \left(\frac{a_{\odot}}{r_{\odot}} \right)^3 (\alpha^2(1 + 4e^2) + \gamma^2(1 - e^2) - \left(\frac{2}{3} + e^2 \right) + \frac{2\alpha e r_{\odot}}{a}) \quad (3)$$

where α and γ are presented in [5]. The second average is applied with respect to the third body. To do this we perform an average over the true anomaly of the disturbing body, (f_{\odot}) in Eqs. (2) and (3). Thus, we obtain the double average disturbing potential given by

$$\begin{aligned} R_{3b+SRP} = & \langle \langle R_{3b} \rangle \rangle + \langle \langle R_{SRP} \rangle \rangle = \frac{15}{32} n_M^2 (\beta - 1) a^2 (1/2 e^2 (\cos(i_{\odot}) - 1) \times \\ & (\cos(i_{\odot}) + 1) (\cos(i) - 1)^2 \cos(2\Omega - 2\Omega_{\odot} - 2w) + 1/2 e^2 (\cos(i_{\odot}) - 1) (\cos(i_{\odot}) + 1) \times \\ & (\cos(i) + 1)^2 \cos(2\Omega - 2\Omega_{\odot} + 2w) + 2 \sin(i) \sin(i_{\odot}) e^2 \cos(i_{\odot}) (\cos(i) - 1) \times \\ & \cos(-2w + \Omega - \Omega_{\odot}) + 2 \sin(i) \sin(i_{\odot}) e^2 \cos(i_{\odot}) (\cos(i) + 1) \cos(2w + \Omega - \Omega_{\odot}) - \\ & 3/5 (\cos(i) + 1) (\cos(i_{\odot}) + 1) (\cos(i_{\odot}) - 1) (\cos(i) - 1) (e^2 + 2/3) \cos(2\Omega - 2\Omega_{\odot}) - \\ & \frac{12}{5} \sin(i) \cos(i_{\odot}) \cos(i) (e^2 + 2/3) \sin(i_{\odot}) \cos(\Omega - \Omega_{\odot}) + (((\cos(i))^2 - 1) (\cos(i_{\odot}))^2 + \\ & 2 (\sin(i))^2 (\sin(i_{\odot}))^2 + (\cos(i))^2 - 1) e^2 \cos(2w) - 3/5 (e^2 + 2/3) (((\cos(i))^2 + 1) \times \\ & (\cos(i_{\odot}))^2 - 5/3 + 2 (\sin(i))^2 (\sin(i_{\odot}))^2 + (\cos(i))^2)) (1 - e_{\odot}^2)^{-3/2} \end{aligned} \quad (4)$$

Note that the inclination and the longitude of the ascending node of the disturbing body orbit (Sun, $i_{\odot}, \Omega_{\odot}$) appear in Eq. (4) because it is considering that this body is in

a elliptical and inclined orbit. The argument of pericentre the Sun (w_{\odot}) does not appear in this equation because of the application of the second average which eliminates the short-period terms and also the argument of pericentre of the disturbing body.

2.2 Non-uniform distribution of mass of Mercury

For the perturbations due to nonuniform distribution of mass of the planet is taken into account the simplified model presented by [1]. Thus, considering the equatorial plane of Mercury as the reference plane, we obtain the disturbing potential given by [1]

$$\langle\langle R_{J2} \rangle\rangle = -\frac{1}{4} \frac{\epsilon n^2 (-2 + 3 \sin^2(i))}{(1 - e^2)^{3/2}} \tag{5}$$

where $\epsilon = J_2 R_M^2$ and R_M is the equatorial radius of Mercury. Were $\epsilon_1 = J_3 R_M^3$.

$$\langle\langle R_{J3} \rangle\rangle = -\frac{3}{8} \frac{\epsilon \epsilon_1 n^2 \sin(i) (-4 + 5 \sin^2(i)) \sin(w)}{(1 - e^2)^{5/2} a} \tag{6}$$

3 Results

In this section we present the results obtained when we consider the perturbation of the third body, the non-spherical shape of the central body and the solar radiation pressure. The disturbing potential R (Eqs. (4), (5) and (6)) is given by

$$R = \langle\langle R_{J2} \rangle\rangle + \langle\langle R_{J3} \rangle\rangle + \langle\langle R_{3b+SRP} \rangle\rangle. \tag{7}$$

Replacing Eq. (7) in the Lagrange planetary equations and numerically integrated the set of nonlinear differential equations using the software Maple to obtain the variation of orbital elements over time. Emphasis is given for frozen orbits, which are orbits what keep constant or almost constant the following orbital elements: eccentricity, inclination and argument of pericentre of the solar sail. In [4] is presented the necessary and sufficient conditions for using solar sails in order to reduce the effects of perturbations due to external forces received by a satellite.

However, to have frozen orbits, we have to solve the equation $dw/dt = 0$, which depends on three variables, namely, e , i , and a . This equation represents a 3-D surface which is shown in Fig. 1(a). Points on this surface are initial conditions of frozen orbits. Note that for low altitude orbits the central region of figure representing the frozen orbits is obtained for the value of $w = 270$ degrees and larger values of eccentricity. In order to enter into more details, we make the section for a fixed value of the semi-major axis, for instance, $a = 3500$ km, which corresponds to low altitude orbits. For this value we plot the curve e versus i in Fig. 1(b). We can see from it that we find families of frozen orbits, even for large inclinations. The central part of Fig. 1(b) shows the frozen orbits. This orbits arise when $w = 270$ degrees as shown in Fig. 1(b), but when $w = 90$ degrees, do not get frozen orbits.

As an application of the results, let us consider the case with $i = 90^\circ$, and some eccentricity values as shown in the figure legends. The behavior of artificial satellites

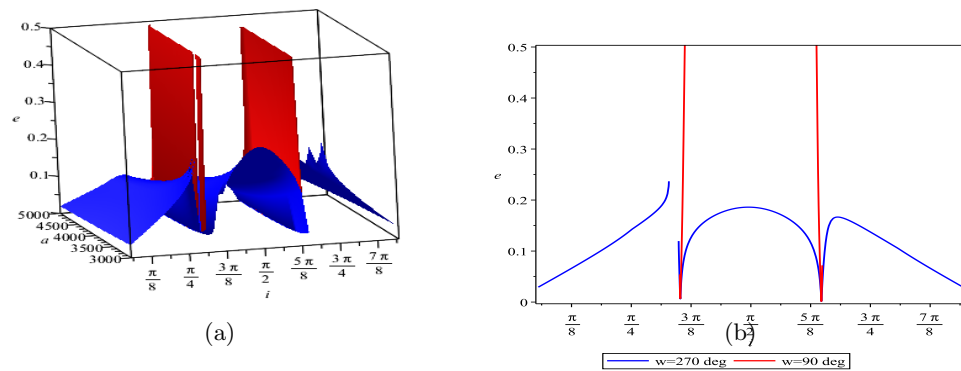


Figure 1: Section of frozen orbits with, $J_2 = 6 \times 10^{-5}$, $J_3 = J_2/2$ and $\beta = 0.2$. Frozen orbits on the central part. (a) Section (a, i, e) of frozen orbits. (b) Section (i, e) of frozen orbits with $a = 3500$ km.

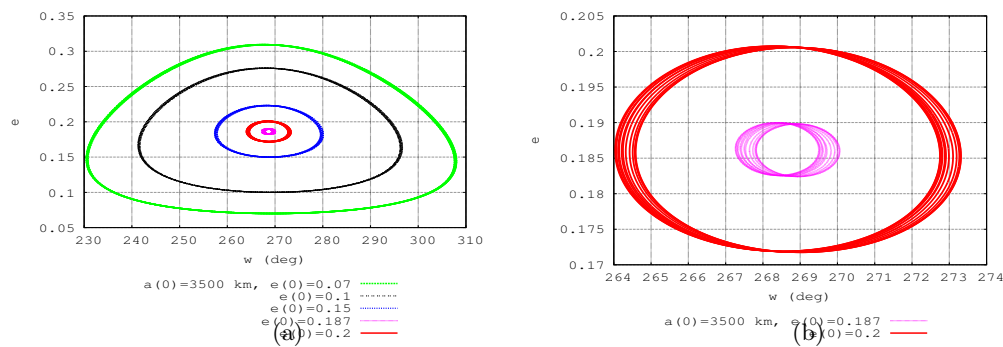


Figure 2: Integrations of the Lagrange planetary equations. Section of frozen orbits with $a = 3500$ km, $i = 90^\circ$, $J_2 = 6 \times 10^{-5}$, $J_3 = J_2/2$ and $\beta = 0.2$. (a) $e \times w$. (b) $e \times w$ (zoom).

around Mercury is analyzed for some particular cases. This task is done by using the software Maple to numerically integrate the set of nonlinear differential equations given by Eq. (7). Then, for these initial conditions, we plot a diagram w versus e in Fig. 2(a) and Fig. 2(b). From those figures, we deduce that the eccentricity $e = 0.187$ is a strong candidate for frozen orbits. Looking at Fig. 2(a) we obtain frozen orbit that librates around the equilibrium point for $w = 270$ degrees. Note that different amplitudes are presented and the one with less variation of the orbital elements are selected as suggestions for future space missions of a solar sail around Mercury. Looking at Figs. 2(a) and 2(b) we found orbits who present lower variation of the orbital elements. Using the values from eccentricity obtained in Figs. 2(a) and 2(b), those with less amplitude variation, and making a plot of eccentricity with respect to time (see Fig. 3(a)). We show that the frozen orbit where $e = 0.187$ presents a smaller amplitude of variation compared with the orbit where $e = 0.2$. Fig. 3(b) shows the behavior of the pericentre position with respect to

time. This figure shows that the orbit with eccentricity 0.187 is well behaved compared to the orbit where the eccentricity is 0.2. Note that the orbit with $e = 0.07$ collides with the surface of Mercury, because in this case, the orbit intersects the mean radius of the planet. Fig. 2(a) shows that the orbit with $e = 0.07$ librates around the equilibrium point, but with large amplitude, so the satellite's eccentricity grows and collides with the surface of Mercury as shown in Fig. 3(b).

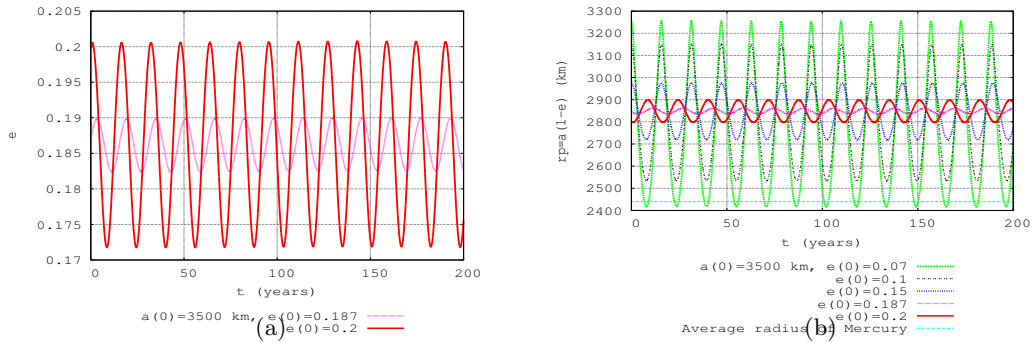


Figura 3: Frozen orbits with $a = 3500$ km, $i = 90^\circ$, $J_2 = 6 \times 10^{-5}$, $J_3 = J_2/2$ and $\beta = 0.2$. (a) $e \times t$, (b) $r_p = a * (1 - e) \times t$.

Fig. 4 shows the behavior of the eccentricity for different β values, i.e. different values of the quantity mass/area of the solar sail. When the value of the quantity mass/area is equal to 0.5 the characteristics of the solar sail are unsuitable because they have a greater variation of the eccentricity as shown in Fig. 4. Then, we propose a solar sail with features where the β value is equal to 0.2. Therefore we present a type of satellite that uses sunlight to print a force on the sail to help ensure that the satellite remains in orbit for a longer time with lower costs in orbits correction. The solar sail performance is parameterised by the total artificial satellite mass per unit area m/A , see [3].

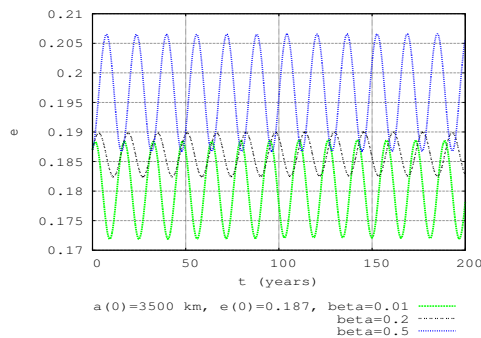


Figura 4: $e \times t$, frozen orbits with $a = 3500$ km, $i = 90^\circ$, $J_2 = 6 \times 10^{-5}$, $J_3 = J_2/2$ and different values of the solar lightness β .

4 Conclusions

In this paper we present the dynamics of a spacecraft, where this vehicle is a solar sail. The perturbations considered in this study are non-spherical shape of the central body, perturbation of the third body and solar radiation pressure. The third body is considered in elliptical and inclined orbit. With the approach used in this work, analyzing the surface of frozen orbit, it was possible to identify frozen orbits, i.e. orbits with small amplitude variation of the orbital elements, in particular eccentricity, inclination and argument of the pericentre. Considering a spacecraft around the Mercury planet with semi-major axis equal to 3500 km we found frozen orbits, in particular an orbit with the following initial conditions $e = 0.187, i = 90^\circ, g = 270^\circ$ and $h = 90^\circ$. This set of initial conditions determines an orbit with an altitude of 405.80 km, which is between the values to be considered in future scientific missions around Mercury. We show that the quantity mass per unit area m/A of the solar sail has a strong influence on the dynamics of the spacecraft, which requires, in mission planning, a careful analysis with respect the quantity mass per unit area m/A of the solar sail. As a continuation of this work a more accurate model for solar radiation pressure must be taken into account, possibly considering the effect of shadow on the solar sail. It should also be analyzed the effect of C_{22} term in the dynamics of the solar sail.

Acknowledgements

Sponsored by CNPq - Brazil. The author is grateful to CNPq- Brazil for contracts 306953/2014-5.

Referências

- [1] J. P. S. Carvalho, R. Vilhena de Moraes and A. F. B. A. Prado, Dynamics of Artificial Satellites around Europa, *Mathematical Problems in Engineering*, vol. 2013, (2013) Article ID 182079.
- [2] M. C. P. Faria, Dinâmica orbital e controle de orientação de um veículo espacial com uma vela solar composta Tese de doutorado em Engenharia e Tecnologia Espacial/Mecânica Espacial e Controle, INPE, (2009).
- [3] C. R. McInnes, *Solar Sailing: Technology, Dynamics and Mission Applications*, Springer-Praxis Series in Space Science and Technology, Springer-Verlag, (1999).
- [4] T. C. Oliveira and A. F. B. A. Prado, Evaluating orbits with potential to use solar sail for station-keeping maneuvers, *Advances in the Astronautical Sciences*, vol. 153, 1699-1718, (2015).
- [5] E. Tresaco, A. Elipe and J. P. S. Carvalho, Frozen orbits computation for a Mercury solar sail. In: 25th AAS/AIAA Space Flight Mechanics Meeting, 2015, Williamsburg, VA. 25th AAS/AIAA Space Flight Mechanics Meeting, (2015).